Molecular architecture of *Manduca sexta* midgut V_1 ATPase visualized by electron microscopy

Michael Radermacher[a], Teresa Ruiz[a], William R. Harvey[b], Helmut Wieczorek[c], Gerhard Grüber[b,c,*]

[a] *Max-Planck-Institut für Biophysik, Abteilung Strukturbiologie, D-60528 Frankfurt am Main, Germany*
[b] *Whitney Laboratory, University of Florida, St. Augustine, FL 32086, USA*
[c] *Universität Osnabrück, Fachbereich Biologie/Chemie, D-49069 Osnabrück, Germany*

Received 4 April 1999; received in revised form 20 May 1999

Abstract The structure of the V_1 ATPase from the tobacco hornworm *Manduca sexta* has been determined from electron micrographs of isolated, negatively stained specimens. The resulting images clearly show a pseudohexagonal arrangement of six equal-sized protein densities, presumably representing the three copies each of subunits *A* and *B*, which comprise the headpiece of the enzyme. A seventh density could be observed either centrally or asymmetrically to the hexamer. The maximum diameter of the V_1 complex in the hexagonal projection is 13 nm with each of the six peripheral densities being 3–4 nm in diameter.

Key words: V_1 ATPase; Electron microscopy; Image processing; *Manduca sexta*

1. Introduction

Proton-motive vacuolar-class ATPases (V-ATPases or V_1V_O-type ATPases) in eukaryotes are commonly associated with membrane-bound organelles other than mitochondria and chloroplasts as well as with certain types of animal plasma membranes [1]. As the name implies, the V_1V_O-type ATPases are composed of two parts: a membrane-embedded, ion-conducting complex, V_O, and an extrinsic complex, V_1, in which ATP hydrolysis takes place [2]. V_1 complexes also occur freely in the cytosol, due to reversible dissociation from the V_1V_O holoenzyme under special physiological conditions as shown in yeast [3] and in the tobacco hornworm *Manduca sexta* [4]. The V_1 complex as isolated from tobacco hornworm midgut exhibits a Ca^{2+}-stimulated ATPase activity and therefore it was termed V_1 ATPase [4].

Cytosolic V_1 ATPase from the tobacco hornworm, which is the object of our studies, comprises the two major catalytic subunits *A* and *B* in a stoichiometry of A_3B_3 and the so-called *stalk* subunits *C*, *D*, *E*, *F* and *G* [5] in a proposed stoichiometry of $C_1:D_1:E_1:F_1:G_3$ with apparent molecular masses of 67, 56, 40, 32, 28, 14 and 16 kDa, respectively [4,6]. The *stalk* subunits appear to link the V_1 and V_O portions as seen in negatively stained electron micrographs of V-ATPase-containing membranes [7]. Low resolution structural studies of the *M. sexta* V_1 ATPase using small-angle X-ray scattering have shown that the enzyme is a highly elongated molecule with a maximal length of about 22 nm. It has a radius of gyration, R_g, of 6.1 nm and a molecular mass of 550 kDa. The X-ray data define a mushroom-shaped V_1 ATPase, which consists of an approximately 14.5 nm headpiece, joined at right angles to an approximately 11 nm stalk [6].

Here, we use electron microscopy to visualize directly the structure of the V_1 ATPase from *M. sexta*. The averaged EM images reveal six major masses of density as a pseudohexagon that surround a central cavity containing an interior protein density.

2. Materials and methods

2.1. Protein isolation and analysis

The V_1 ATPase from *M. sexta* midgut was isolated according to Gräf et al. [4]. Protein concentrations were determined with amido black [8]. SDS-polyacrylamide gel electrophoresis was performed with 17.5% total acrylamide and 0.4% cross-linked acrylamide. Protein bands on gels were stained with Coomassie brilliant blue R [9]. ATPase activity was measured as described previously [8].

2.2. Electron microscopy and two-dimensional image analysis

For electron microscopy the protein was diluted in 20 mM Tris-HCl (pH 8.1) and 150 mM NaCl. The sample was applied to 400 mesh copper grids using the carbon sandwich technique [10] with 0.5% uranyl acetate as a negative stain. Micrographs were recorded on a Philips CM 120 electron microscope, at 120 kV with an instrumental magnification of 60 000×, and an electron dose of approximately 10 $e^-/Å^2$. The negatives were scanned on a flat-bed SCAI (Zeiss) microdensitometer with 7 μm pixel size, which was subsequently reduced by binning to a pixel size of 21 μm. For image processing the SPIDER software [11] with extensions and XMIPP [12] were used. Images of 4765 single particles were windowed from 10 micrographs, normalized in contrast and aligned (e.g. [13]). Correspondence analysis [14,15], as well as the technique of self-organizing maps [16,17], was applied to assess the consistency of the data set. The resolution was calculated using the Fourier ring correlation criterion FRC_5 (five times over noise correlation) [18–20].

3. Results and discussion

3.1. Isolation and characterization of the V_1 ATPase

The experiments described here utilize V_1 ATPase of the larval *M. sexta* midgut consisting of at least seven subunits, designated *A*, *B*, *C*, *D*, *E*, *F* and *G* as shown by SDS-PAGE analysis of the isolated complex (Fig. 1A). The enzyme activity was approximately 2 μmol ATP hydrolyzed per mg protein per min. Electron micrographs of negatively stained samples (Fig. 1B) show a highly monodisperse distribution of the V_1 ATPase.

*Corresponding author. Fax: (49) (541) 969 3503.
E-mail: ggrueber@biologie.uni-osnabrueck.de

Abbreviations: PAGE, polyacrylamide gel electrophoresis; SDS, sodium dodecyl sulfate

PII: S0014-5793(99)00739-5

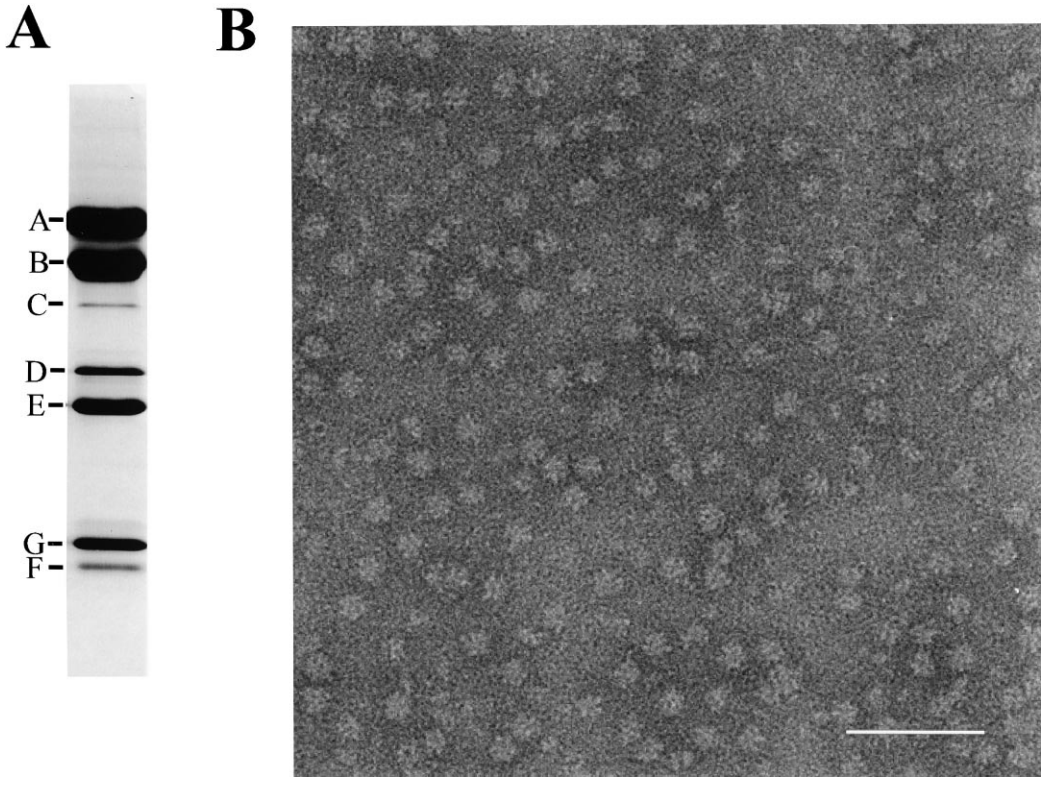

Fig. 1. SDS-PAGE of isolated V_1 ATPase (A) and an electron micrograph of negatively stained V_1 ATPase (B) from *M. sexta* larval midgut. A: 10 μg V_1 ATPase was applied to an SDS-polyacrylamide gel and the subunits were stained with Coomassie blue. B: Bar represents 200 nm.

3.2. Averaged views of the V_1 complex

An average of the V_1 ATPase calculated from the complete set of 4765 images (Fig. 2A) shows a pseudohexagonal arrangement of six protein densities with an overall diameter of approximately 13 nm. This is in agreement with the shape of the V_1 ATPase determined recently by X-ray small-angle scattering, which likewise showed six major masses of density that were grouped in a pseudohexagonal arrangement with a diameter of approximately 14.5 nm [6]. In both cases the six masses can be interpreted as three copies each of subunits *A* and *B* arranged in an alternating manner. The center of the particle shows a lower density yet does not appear hollow and would be consistent with the presence of a central *stalk*. The stalk had previously been predicted, by X-ray small-angle scattering, to have a length of approximately 11 nm and to provide sufficient space for the smaller V_1 sub-

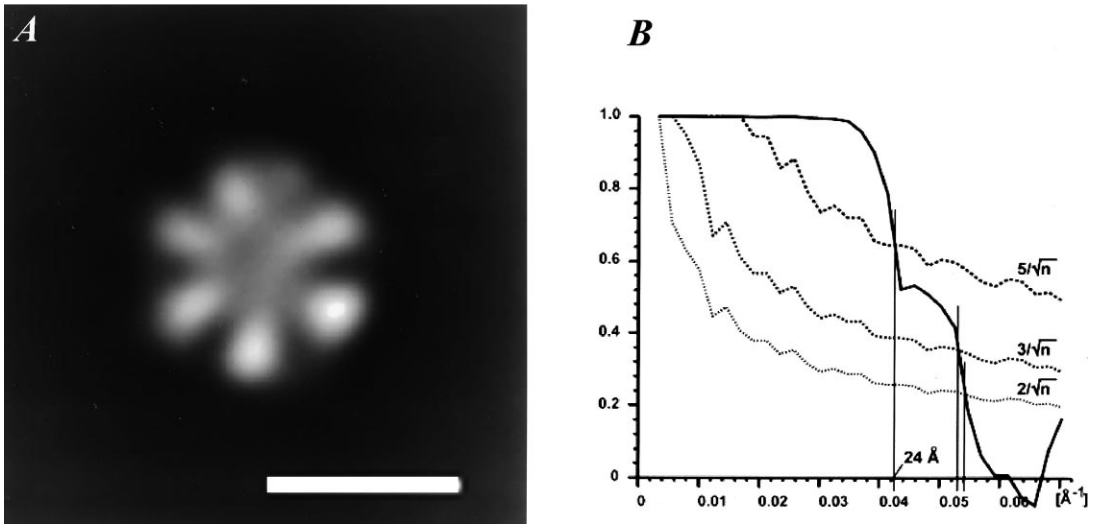

Fig. 2. A: Average image of the V_1 ATPase calculated from all 4765 particles. Bar represents 10 nm. B: Fourier ring correlation curve (solid line) and noise correlation reference curves ($5/\sqrt{N}$ for FRC_5, $3/\sqrt{N}$ for FRC_3 and $2/\sqrt{N}$ for FRC_2). The resolution of the average was determined to be 2.4 nm using the FRC_5 criterion (between 1.8 and 1.9 nm for FRC_3 and FRC_2). The average shown in A is low-pass filtered to the resolution of 2.4 nm.

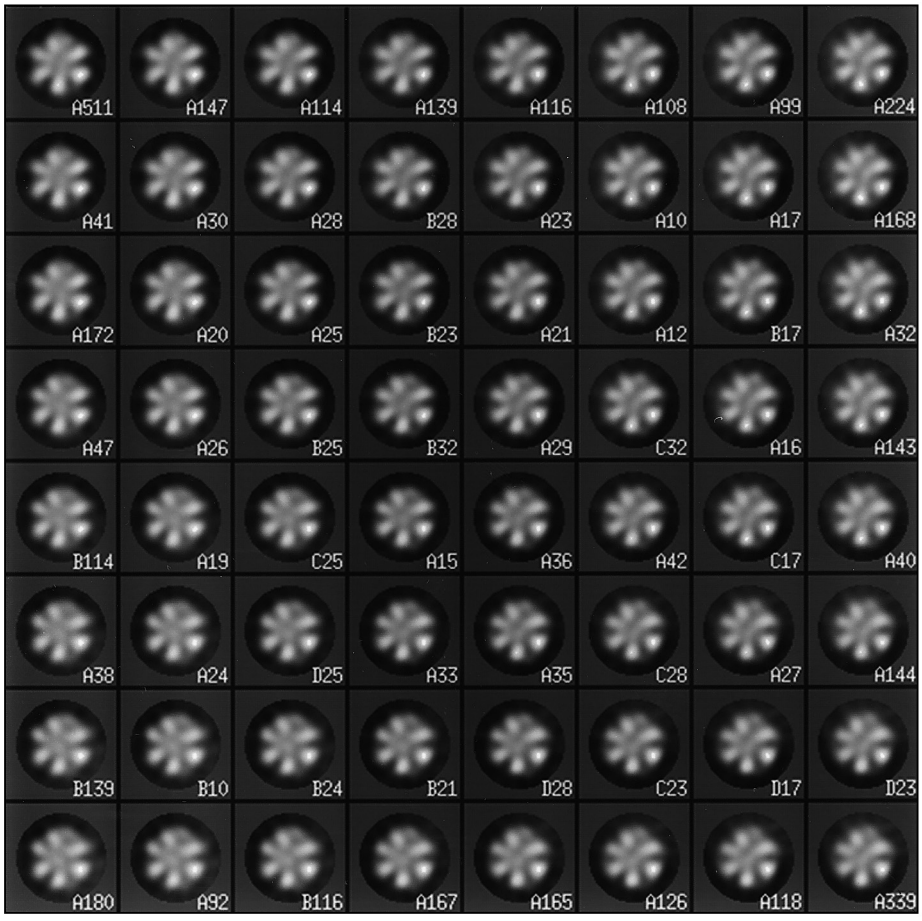

Fig. 3. Map obtained by applying the method of self-organizing maps (neural networks) to the image set. Seen are the nodes that represent the image set. Numbers indicate the number of images that contribute to each node. The map gives an overview over the variations in the set of images. The image in the upper left corner matches closely the overall average. In the lower left corner a view can be observed that shows a higher density in the center of the particle. The variations seen in this map can most easily be explained by continuous variations of the particle orientations (rocking) in the specimen plane.

units *C*, *D*, *E*, *F* and *G* [6]. Near one of the outer densities an additional mass can be observed, which breaks the apparent six-fold symmetry. This may be caused by small tilts of the V_1 ATPase perpendicular to its hexagonal axis, sufficient to displace the central mass without apparent distortion of the outer hexagon. Preliminary, three-dimensional reconstruction of this V_1 ATPase indicates that this mass lies just below the A_3B_3 hexamer (unpublished data). The resolution of the averaged image was 2.4 nm, as determined by Fourier ring correlation FRC_5 (1.8 nm with FRC_2) [18–20] (Fig. 2B).

The structural feature of a hexagonal arrangement of the A_3B_3 subcomplex and an asymmetrically placed seventh mass is reminiscent of the subunit arrangement of the closely related F-ATPases [21,22]. Analysis of images of the F_1 ATPase from *Escherichia coli* showed that the major subunits α and β are arranged as a hexagonal barrel with an additional off-centered density that has been shown, by difference maps and monomaleimido gold labeling, to include the stalk subunits γ and ε [23–25].

Correspondence analysis [14,15], using eight factors, was applied to analyze the variability of the data set. This procedure reduces the dimensionality of the data set and describes the variation of major features among the whole of images. Each image is represented as a point in an eight-dimensional space. Points close to each other represent similar images whereas a large distance between two points indicates a large difference between two images. No distinct pattern of classes could be found, either in two-dimensional projections of this eight-dimensional space or with the aid of classification techniques. A self-organizing map [16,17] was calculated using a neural network approach to obtain an overview over the variations present in the data set (Fig. 3). Most of the variations seen can be explained with a rocking behavior of the molecule around its preferred orientation. In the upper left corner (Fig. 3) the image with the most members strongly resembles the overall average (Fig. 2A). In the lower left corner a view can be seen that shows a higher central density indicating the presence of a central mass.

Taken together, the structural data presented in this paper support the hexagonal arrangement of the *A* and *B* subunits of the *M. sexta* V_1 ATPase and show the existence of a seventh mass observed either centrally or asymmetrically to the hexamer. In the near future electron microscopical images of this complex labeled with monoclonal antibodies against the subunits *A* and *B* may confirm their alternating arrangement in the enzyme. Furthermore, labeling with antibodies to *C*, *D*, *E*, *F* and *G* subunits may reveal their spatial arrangement in

the *stalk* subunits and thus provide the basis for exploring their function.

Acknowledgements: This research was supported by the Deutsche Forschungsgemeinschaft (Wi698 and SFB 431), by National Institutes of Health Grant A1 22444, and the NSF Grant DBI-9515518.

References

[1] Harvey, W.R. and Wieczorek, H. (1997) J. Exp. Biol. 200, 203–216.
[2] Nelson, N. (1992) Curr. Opin. Cell Biol. 4, 654–660.
[3] Kane, P.M. (1995) J. Biol. Chem. 270, 17025–17032.
[4] Gräf, R., Harvey, W.R. and Wieczorek, H. (1996) J. Biol. Chem. 271, 20908–20913.
[5] Tomashek, J.J., Graham, L.A., Hutchins, M.U., Stevens, T.H. and Klionsky, D.J. (1997) J. Biol. Chem. 272, 26787–26793.
[6] Svergun, D.I., Konrad, S., Huß, M., Koch, M.H.J., Wieczorek, H., Altendorf, K., Volkov, V.V. and Grüber, G. (1998) Biochemistry 37, 17659–17663.
[7] Dschida, W.J. and Bowman, B.J. (1992) J. Biol. Chem. 267, 18783–18789.
[8] Wieczorek, H., Cioffi, M., Klein, U., Harvey, W.R., Schweikl, H. and Wolfersberger, M.G. (1990) Methods Enzymol. 192, 608–616.
[9] Schweikl, H., Klein, U., Schindlbeck, M. and Wieczorek, H. (1989) J. Biol. Chem. 264, 11136–11142.
[10] Tischendorf, G.W., Zeichhardt, H. and Stöffler, G. (1974) Mol. Gen. Genet. 134, 187–208.
[11] Frank, J., Radermacher, M., Penczek, P., Zhu, J., Li, Y., Ladjadj, M. and Leith, A. (1996) J. Struct. Biol. 11, 190–199.
[12] Marabini, R., Masegosa, I.M., San Martin, M.C., Marco, S., Fernández, J.J., de la Fraga, L.G., Vaquerizo, C. and Carazo, J.M. (1996) J. Struct. Biol. 116, 237–240.
[13] Frank, J. and Radermacher, M. (1986) in: Advanced Techniques in Biological Electron Microscopy (Koehler, J.K., Ed.), Vol. III, pp. 1–72, Springer Verlag, Heidelberg.
[14] van Heel, M. and Frank, J. (1981) Ultramicroscopy 6, 187–194.
[15] Frank, J. and van Heel, M. (1982) J. Mol. Biol. 161, 134–137.
[16] Kohonen, T. (1990) Proc. IEEE 78, 1464–1480.
[17] Marabini, R.C.J.M. (1994) Biophys. J. 66, 1804–1814.
[18] Saxton, W.O. and Baumeister, W. (1982) J. Microsc. 127, 127–138.
[19] van Hell, M., Keegstra, W., Schutter, W. and van Bruggen, E.J.F. (1982) in: Life Chemistry Reports, Suppl. 1, The Structure and Function of Invertebrate Respiratory Proteins. EMBO Workshop, Leeds (Wood, E.J., Ed.), pp. 69–73.
[20] Radermacher, M. (1988) J. Electron Microsc. Tech. 9, 359–394.
[21] Boekema, E.J., Berden, J.A. and van Heel, M.G. (1986) Biochim. Biophys. Acta 851, 353–360.
[22] Gogol, E.P., Lücken, U., Bork, T. and Capaldi, R.A. (1989) Biochemistry 28, 4709–4716.
[23] Gogol, E.P., Aggeler, R., Sagermann, M. and Capaldi, R.A. (1989) Biochemistry 28, 4714–4724.
[24] Wilkens, S. and Capaldi, R.A. (1992) Arch. Biochem. Biophys. 299, 105–110.
[25] Wilkens, S. and Capaldi, R.A. (1994) Biol. Chem. Hoppe-Seyler 375, 43–51.